Available online at www.sciencedirect.com
SCIENCE DIRECT®
Chemical Physics Letters 366 (2002) 449–457
CHEMICAL PHYSICS LETTERS
www.elsevier.com/locate/cplett

Calculating quasi-bound rotation-vibrational states of HOCl using massively parallel computers

Hamse Y. Mussa [a], Jonathan Tennyson [b,*]

[a] Unilever Centre, Department of Chemistry, University of Cambridge, Lensfield Road, Cambridge CB2 1EW, UK
[b] Department of Physics and Astronomy, University College London, Gower Street, London WC1E 6BT, UK

Received 31 January 2002; in final form 20 September 2002

Abstract

We calculate positions and predissociation widths for quasi-bound states of HOCl with total angular momentum of $J = 0$ and $J = 3$. An ab initio potential energy surface is used in conjunction with a complex absorbing potential (CAP). These calculations are performed by diagonalising a complex symmetric Hamiltonian using our discrete variable representation (DVR) based parallel code, PDVR3D, and a truncation and diagonalisation algorithm. The resonances are identified as those states in the continuum, which are stable with respect to CAP and basis set parameters. Test on the resonances are carried out using over 90 different absorbing potential heights. Resonances of both Feshbach (vibrational trapping) and shape (rotational trapping) are identified.

1. Introduction

A quasi-bound (resonance) state can be defined as a long-lived state of a system which has sufficient energy to break up into fragments [1]. In other words resonances are localised states in the continuum of the solution of the Schrodinger equation for a system with $E > 0$. This phenomenon is common, and often plays and important role in energy transfer processes such as scattering and unimolecular reactions. For instance, the rate of unimolecular dissociation of an excited molecule $(ABC)^*$ into A + BC fragments can be controlled by the lifetime of the quasi-bound states.

For simple systems there are two physically distinct ways of trapping quasi-bound states which lead to the formation of Feshbach and shape resonance. For nuclear motion problems, Feshbach resonances involve the trapping of energy in vibrational degrees of freedom which are not dissociative. Dissociation occurs via intramolecular vibrational redistribution (IVR). For systems moving on a single potential energy surface, these resonances only occur for triatomic or larger molecules but can be found for all angular momentum states including $J = 0$. Conversely shape resonances are caused by the trapping of states behind a centrifugal barrier and thus can occur for diatomics, but only for states with $J > 0$. Shape

* Corresponding author. Fax: +44-20-7679-2564.
E-mail address: j.tennyson@ucl.ac.uk (J. Tennyson).

0009-2614/02/$ - see front matter
PII: S0009-2614(02)01554-3

resonances decay by tunneling through the centrifugal barrier.

So far all theoretical studies on quasi-bound states of strongly bound triatomics have concentrated on resonances of the Feshbach type. However it has long been established, at least for H_3^+, that shape resonances are observable and numerous [2]. In this case Feshbach resonances are much too short-lived to explain the observed near-dissociation spectrum [3].

Theoretically quasi-bound states can be accurately calculated as the poles of the scattering matrix. However, this is a difficult task which can be computationally demanding for even simple systems with three atoms. Fortunately the quasi-bound nature of resonances makes them suited to L^2 methods. Employing L^2 complex methods such as complex scaling [1] and complex absorbing potential (CAP) [4], one can transform the Hamiltonian representing resonances to an L^2 non-Hermitian effective Hamiltonian operator. The energy of the poles are then obtained by diagonalising the effective Hamiltonian.

Using the CAP method in time-independent calculations, several different groups [5–12] have reported vibrational quasi-bound states (Feshbach resonances) for triatomic systems. Skokov and Bowman [13] recently reported calculations, in which the Coriolis coupling was ignored, on resonances of rotating HOCl for $J > 1$. Other studies of resonances with $J > 0$ have been reported for HCO [14–18], HNO [19] and recently HOCl [20]. In particular we note that Weiss et al. [17] found that Coriolis coupling is essential for determining the lifetimes of the vibrational states with $K = 0$. However all these works cited above concentrate on rotationally excited Feshbach resonances.

Performing exact rotation–vibration calculations which extend all the way to dissociation remains a difficult and computationally demanding problem without the extra complication of resonances for which total angular momentum, J, is greater than 1. The characterisation of states with $J > 1$ above dissociation is the problem that we address in this article. In order to meet this challenge we have adapted our methods which have served well at low, medium and high energies on computers with massively parallel processors [21] to the resonance problem by using a CAP. Here we present resonance parameters for HOCl with $J = 0$ and $J = 3$ calculated using the ab initio potential energy surface due to Skokov et al. [22]. For $J = 0$ the results are directly comparable with the result of Skokov et al. [6] who used this problem as a benchmark to compare different L^2 methods of calculating resonance parameters.

HOCl plays a crucial role in ozone destruction in the stratosphere. Although it is a short-lived chlorine reservoir, its rapid photolysis to produce Cl can catalyse the conversion of other Cl reservoirs such as $ClONO_2$, which are inactive, to active Cl. This heightens the effectiveness of Cl in the destruction of ozone. Therefore theoretical study of the photo/unimolecular dissociation of the molecule can enhance our understanding of the HOCl role in the ozone depletion. This problem, and the role of resonances in it, has been the subject of a number recent experimental, spectroscopic studies, see [23] and references therein.

2. Method

Our adaptation of the discrete variable representation (DVR) program DVR3D [24] to run on massively parallel computers, known as PDVR3D, has been documented elsewhere [21,25]. This program has been successfully used to obtain rotation–vibration states up to dissociation, see for example [26], where particular use has been made of its near linear computational scaling with J for problems with low-rotational excitation.

In this work we use Jacobi co-ordinates (R, r, θ), where R is the dissociation co-ordinate, distance of Cl from the centre of mass of OH, r is the OH internuclear distance and θ is the angle between **R** and **r**. For the ro-vibrational motion states we use a body-fixed axis system which places z-axis along **R**. We denote the projection of the total angular momentum, J, on this z-axis as k.

The essence of the CAP method is the introduction of an absorbing potential iU, which is a function of the dissociation co-ordinate, to the system in the asymptotic region of the real potential V. Hence the effective Hamiltonian which

represents the quasi-bound system can be written as

$$\hat{H}' = \hat{H} - iU(R), \tag{1}$$

where $\hat{H}$ is the usual L^2 real Hamiltonian operator. The CAP used here and elsewhere is given by

$$\begin{aligned} U &= \lambda\left(\frac{R - R_{\min}}{R_{\max} - R_{\min}}\right)^n, \quad R > R_{\min} \\ U &= 0, \quad R \leqslant R_{\min}, \end{aligned} \tag{2}$$

where λ is the height of the absorbing potential, and $R_{\min}$ and $R_{\max}$ define the range of the absorbing potential. Following Skokov et al. [6], we use $n = 3$. The absorbing potential makes $\hat{H}'$ an L^2 complex symmetric Hamiltonian which satisfies

$$\hat{H}'\psi_n = \left(E_n - \mathrm{i}\frac{\Gamma_n}{2}\right)\psi_n, \tag{3}$$

where E_n is the resonance position, and Γ_n is the width (inverse lifetime) of the nth resonance state.

To obtain the complex eigen-pairs ($E_n - \mathrm{i}(\Gamma_n/2)$ and ψ_n), $\hat{H}'$ is represented in a basis set and then diagonalised. Riss and Meyer [27] showed that, despite the artificial perturbation induced by the absorbing potential, if $\hat{H}'$ is projected on complete basis set, the exact resonance state eigen-pairs $(E_n - \mathrm{i}(\Gamma_n/2), \psi_n)$ can be obtained in the limit $\lambda \to 0$. In practice the eigenfunctions of $\hat{H}'$ can only be represented by a finite basis. In a finite basis representation it is necessary to use a finite λ to localize the eigenfunctions (i.e, to reduce the basis set error). However the artifact introduced by a particular complex absorbing potential form increases with λ [27]. Hence, in the CAP method, the best estimate of the exact resonance state depends on λ. To find the optimal λ (λ_{op}) at which the finite basis (fb) error cancels with the error due to use of finite λ, the $\hat{H}'$ is diagonalised for a set of λ values. As the errors are out of phase, at λ_{op} $\left|(\mathrm{d}E_n^{\mathrm{fb}}/\mathrm{d}\lambda)\right|$ should be a minimum and the complex eigenvalue $E_n^{\mathrm{fb}}(\lambda_{\mathrm{op}})$ for λ_{op} is the best estimate to the exact resonance $(E_n - \mathrm{i}(\Gamma_n/2))$.

2.1. $J = 0$

For $J = 0$ the matrix elements of the complex Hamiltonian can be written as

$$\langle \phi^n_{\alpha\beta\gamma}|\hat{H}'|\phi^m_{\alpha\beta\gamma}\rangle = e_n\delta_{nm} - \mathrm{i}\lambda\langle \phi^n_{\alpha\beta\gamma}|U(R_\beta)|\phi^m_{\alpha\beta\gamma}\rangle, \tag{4}$$

where γ, α and β are the grids points of the DVR basis functions in θ, r and R, respectively. ϕ^n and e_n are the eigenfunctions and eigenvalues of the real vibrational Hamiltonian $\hat{H}$.

Within a DVR, Eq. (4) can be simplified further to

$$\langle \phi^n_{\alpha\beta\gamma}|\hat{H}'|\phi^m_{\alpha\beta\gamma}\rangle = e_n\delta_{nm} - \mathrm{i}\lambda\sum_{\alpha\beta\gamma}\phi^n_{\alpha\beta\gamma}\phi^m_{\alpha\beta\gamma}U(R_\beta). \tag{5}$$

2.2. $J > 0$

We use the two-step variational approach of Tennyson and Sutcliffe [28] to deal with the real ro-vibrational case. The basic idea of the two-step approach is to first solve a series of problems for which k, is assumed to be a good quantum number, i.e., the Coriolis coupling is neglected. There are $J + 1$ $(k = 0, 1, \ldots, J)$ such 'vibrational' problems for the even (i.e., $p = 0$) rotational parity, the parity examined in this work. For computational reasons [29], the selected DVR 'vibrational' wavefunctions are transformed back to finite basis representation (FBR) in θ, i.e, to associated Legendre polynomials $|j, k\rangle$. This angular back transformation can be written [24]

$$C^{nk}_{j\alpha\beta} = \sum_\gamma T^\gamma_j \phi^{nk}_{\gamma\alpha\beta}, \tag{6}$$

where T^γ_j is the transpose of the normal DVR transformation matrix [24].

The second step constructs the fully coupled ro-vibrational Hamiltonian matrix using M of the eigenfunctions $C^{nk}_{\alpha\beta j}$'s as a basis. The ro-vibrational Hamiltonian matrix is diagonalised yielding $(J + 1) \times M$ eigenvectors, D. L of those are then projected on to the 'vibrational' wavefunctions to give the ro-vibrational eigenfunctions for a given total angular momentum and parity

$$|l\rangle = \sum_k \sum_n D^l_{kn} C^{nk}_{j\alpha\beta}. \tag{7}$$

Finally the L selected eigenfunctions, $|l\rangle$, and their corresponding eigenvalues e_l, are used to calculate the matrix elements of the ro-vibrational non-hermitian matrix

$$\langle l'|\hat{H}'|l\rangle = e_l\delta_{ll'} - \mathrm{i}\lambda\langle l'|U(R_\beta)|l\rangle \quad (8)$$

for which the quadrature approximation can also be used in the R coordinate.

3. Calculations

The calculations for resonances states were performed using the potential energy surface (PES) of Skokov et al. [22]. This surface has a dissociation threshold of $D_0 = 19289.2$ cm^{-1} which agrees well with the experimental value of 19289.6 cm^{-1} [30]. It supports about 800 vibrational states. Using this PES Skokov et al. [6] were able to reproduce HOCl experimental vibrational energies up to $7\nu_{\mathrm{OH}}$ (21716.33 cm^{-1}) which is well above its dissociation threshold. This makes the surface ideal for studying quasi-bound states in unimolecular dissociation.

Both $J = 0$ and $J > 0$ problems were solved using DVR in each co-ordinate based on formulations briefly described in Section 2, but well documented elsewhere [21,24,28]. In this formulation, the angular DVR functions are based on the (associated) Legendre polynomials and the radial DVR functions based on Morse oscillator-like functions. In this work the primitive DVR basis were $N_\beta = 96$, $N_\alpha = 45$, and $N_\gamma = 60$ DVR functions in R, r, and θ, respectively. The variational parameters of the Morse-like functions, r_e, ω_e, and D_e, were optimised for the two radial motions [24]. For r they were set to 4.8295 a_0, 0.01654 E_h, and 0.0023 E_h, respectively; for R to 8.980 a_0, 0.00008 E_h, and 0.0000554 E_h [28]. Note that the R grid was designed to extend significantly into the asymptotic region. For this grid, tests were also performed for $N_\beta = 80$ and 120 but, except for large values of $R_{\min}$ (see below) the results obtained with 96 grid points were found to be stable.

The solutions to the real Hamiltonian were found using sequential truncation and diagonalisation [24]. The final size of the 'vibrational' Hamiltonian matrix was truncated to $96 \times N$ with $N = 100$–180, and diagonalised on 96 processors on a massively parallel Cray-T3E computer. The lowest eigen-pairs were saved on disk. For $J > 0$, this process was repeated for each k.

In the second step a fixed number of eigen-pairs from each fixed-k calculation were used to construct the full, real ro-vibrational Hamiltonian matrix which explicitly includes the Coriolis coupling. This Hamiltonian was diagonalised to give a basis for solving the final, complex Hamiltonian, Eq. (8). For this step, eigen-pairs representing low-lying bound states and high-lying states were discarded from the calculation.

For the CAP, we carried out a large number of tests with $R_{\min}$ in the range 10.0 a_0–12.0 a_0 and $R_{\max}$ was set to 14.0 a_0. As discussed in Section 2, λ was varied to find λ_{op} for which $E_n^{\mathrm{fb}}(\lambda_{\mathrm{op}}) \approx E_n - \mathrm{i}(\Gamma/2)$.

Constructing the full Hamiltonian in parallel is quite simple. As only solutions of the real Hamiltonian in the region of dissociation need be used as basis functions for the complex problem, the construction and diagonalisation of the Hamiltonian for a given λ was performed on a single processor meaning that results could be obtained for several values of λ at once by distributing the calculations across the machine. The Hamiltonian matrix was diagonalised using LAPACK complex matrix diagonalisation routine cgeev.

3.1. $J = 0$

The real vibrational Hamiltonian was diagonalised by using sequential diagonalisation truncation approach: for each R grid we solved a 2D Hamiltonian in θ, and r keeping the lowest $N = 150$ eigenfunctions. This reduced the final real 3D Hamiltonian size to 14 400 which was then diagonalised. To test convergence, we repeated the procedure for other 3D-Hamiltonians with sizes of 9600, 11 520, 15 840, and 17 280. The results obtained showed little sensitivity to this choice, for example the resonance widths varied by less than 0.1%, and only results for $N = 150$ are reported.

The $N = 150$ calculations were performed on 96 MPP Cray-T3E processors which took approximately 1.5 h of real time. 2304 eigenfunctions of the 14 400 size matrix were retained. The lowest 480 states were neglected. Tests were performed which used the next 1248, 1430, 1632, and 1824 states to construct the non-hermitian matrix. Again our results are insensitive (less than 0.1%

variation in the resonance widths) to this choice and only results obtained using 1824 states are reported here. To determine $E_n^{\mathrm{fb}}(\lambda_{\mathrm{op}})$, we constructed and diagonalised the non-hermitian matrix for values of λ ranging from 0.00 E_h to 2.06 E_h and for a range of values of $R_{\min}$.

3.2. $J = 3$

To solve this problem, we used the same primitive DVR functions, and parameters, and $N = 100$ for the 'vibrational' matrix size. The following steps outline how the non-hermitian rovibration Hamiltonian was solved:

1. The real 'vibrational' problem was solved in the same fashion as the $J = 0$ Hamiltonian but repeated four times for $k = 0$, 1, 2, 3. For each k the lowest 1920 eigenfunctions were retained.
2. The chosen eigenfunctions were used as a basis set for constructing the fully coupled real ro-vibrational Hamiltonian which results in a matrix of size 7680. Its diagonalisation gave 7680 L^2 eigenfunctions. The term values between 18 700 and 22 300 cm^{-1}, either 3072 or 3456 states in total starting at state 2800, were selected. Again our results show little sensitivity to this choice and the larger value is used for the results reported below.
3. The selected states were used as a basis, see Eq. (8), to construct the non-Hermitian rovibrational Hamiltonian which was then diagonalised.
4. Step three was repeated over 90 times for different values of λ, similar to those used for the $J = 0$ calculations.
5. The resonance positions and the widths were identified as those which were stable with respect to variation of the height of the absorbing potential.

This process required approximate 6 h on 192 processors of the Cray-T3E.

4. Results

The quasi-bound states were calculated for HOCl for total angular momentum $J = 0$, 1 and 3. We determined the resonance states using both graphical and numerical analysis.

In the graphical method we plotted λ-trajectories of the complex eigenvalues of $\hat{H}'$ in the complex plane. The resonance states were identified as those whose trajectories showed pronounced stabilities [1,27]. The resonance energy of the state was identified as the value of the point where the trajectory was slowest, i.e., $\left|\mathrm{d}E_n^{\mathrm{fb}}/\mathrm{d}\lambda\right|$ was a minimum. Here λ should be the optimal value λ_{op}. Hence $E_n^{\mathrm{fb}}(\lambda_{\mathrm{op}})$ was taken as our best estimate of the resonance energy. Fig. 1 shows resonance energy trajectories of the four lowest $J = 3$ quasi-bound states. For each trajectory an arrow indicates the position of $E_n^{\mathrm{fb}}(\lambda_{\mathrm{op}})$.

In the numerical analysis we inspected how the complex eigenvalues change with λ. For our analysis we used the rate $(E_n^{\mathrm{fb}}(\lambda_{i+1}) - E_n^{\mathrm{fb}}(\lambda_i))/\lambda_{i+1} - \lambda_i$. The state associated with a complex eigenvalue family in which the rate showed stability was identified as a quasi-bound state.

Then, with the justifiable assumption that the rate varies slowly in the vicinity of the resonance energy, $E_n^{\mathrm{fb}}(\lambda_{\mathrm{op}})$ was obtained using this equation

$$\left|\frac{E_n^{\mathrm{fb}}(\lambda_{i+1}) - E_n^{\mathrm{fb}}(\lambda_{\mathrm{op}})}{\lambda_{i+1} - \lambda_{\mathrm{op}}}\right| = \left|\frac{E_n^{\mathrm{fb}}(\lambda_{\mathrm{op}}) - E_n^{\mathrm{fb}}(\lambda_{i-1})}{\lambda_{\mathrm{op}} - \lambda_{i-1}}\right|, \tag{9}$$

i.e.,

$$E_n^{\mathrm{fb}}(\lambda_{\mathrm{op}}) = \frac{E_n^{\mathrm{fb}}(\lambda_{i+1})(\lambda_{\mathrm{op}} - \lambda_{i-1}) + E_n^{\mathrm{fb}}(\lambda_{i-1})(\lambda_{i+1} - \lambda_{\mathrm{op}})}{\lambda_{i+1} - \lambda_{i-1}}. \tag{10}$$

For equal intervals of λ $(\lambda_{\mathrm{op}} - \lambda_{i-1} = \lambda_{i+1} - \lambda_{\mathrm{op}})$, which was the case in this work,

$$E_n^{\mathrm{fb}}(\lambda_{\mathrm{op}}) = \frac{E_n^{\mathrm{fb}}(\lambda_{i-1}) + E_n^{\mathrm{fb}}(\lambda_{i+1})}{2}. \tag{11}$$

In practice for almost all states considered here $E_n^{\mathrm{fb}}(\lambda_{i-1}) = E_n^{\mathrm{fb}}(\lambda_{i+1})$ in the vicinity of the resonance, and visual inspection was sufficient to give reliable results.

To test stability of our results with respect to the CAP parameters, the width of each resonance was analysed as function of $R_{\min}$ and λ. Table 1 presents results for three typical $J = 0$ resonance states. As expected, in all cases the value of λ_{op} increases with $R_{\min}$ for a given basis set. Stable

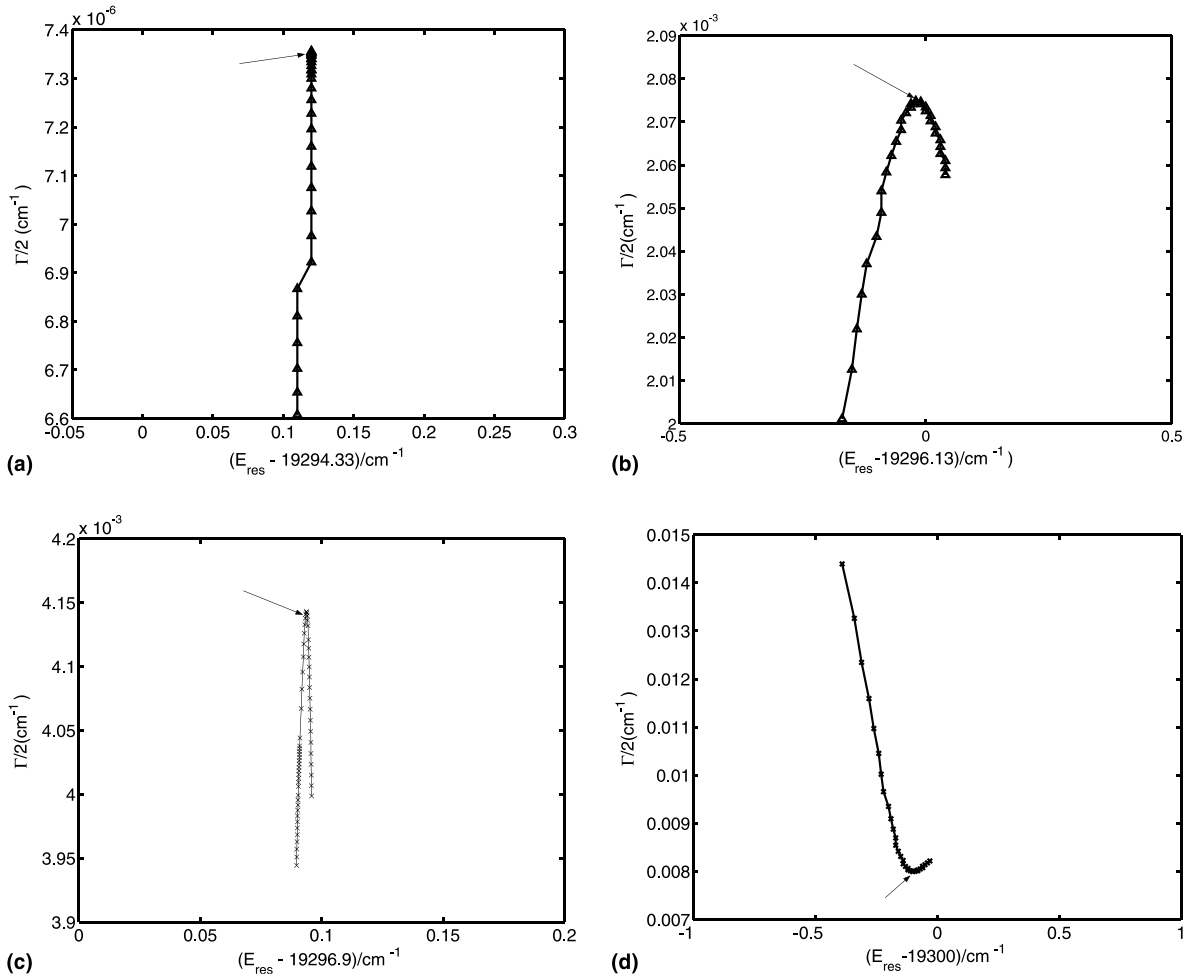

Fig. 1. Resonance positions and widths as a function of λ for the four lowest resonances in the HOCl calculation with $J = 3$, $p = 0$. The arrows show the value of the energy and width (Γ) determined for each resonance.

results are obtained for $R_{\min}$ in the region of 11.0 a_0 and this value is used for the results presented below. However it should be emphasised that the choice of CAP parameters remains the largest source of uncertainty in these calculations.

Table 2 compares our results against those of Skokov et al. [6], who used two different methods to determine their resonance parameters. The resonance energies agree well in all three calculations, but there are notable differences between all three calculations for the widths. Our calculations used larger basis sets than those of Skokov et al. and, as can be seen from the energies, which behave variationally, are better converged. We are confident that this improved convergence means that our estimates for the resonance widths are also more reliable. Thus, for example, Skokov et al. report a width of 0.042 and 0.0042 cm^{-1} for the resonance at 20 194 cm^{-1}. Our calculations give a width significantly narrower, 3×10^{-5} cm^{-1}, than either of these values. Our result is stable to varying $R_{\min}$, λ, the size of the initial basis and the size of the final basis used to diagonalise the complex Hamiltonian. We thus believe that this result represents the true value for the resonance width given by the potential of Skokov et al. [22] and that our more

Table 1
Variation of the resonance widths with R_{min} and λ_{op} for three resonances with $J = 0$

R_{min}/a_0	$E = 19335.86$ (cm^{-1})		$E = 19603.01$ (cm^{-1})		$E = 19905.91$ (cm^{-1})	
	λ_{op}/E_h	Γ (cm^{-1})	λ_{op}/E_h	Γ (cm^{-1})	λ_{op}/E_h	Γ (cm^{-1})
10.50	0.01	0.015	0.01	0.023	0.01	0.013
10.75	0.02	0.011	0.02	0.018	0.02	0.011
11.00	0.07	0.0064	0.04	0.013	0.09	0.0071
11.25	0.09	0.0057	0.12	0.011	0.14	0.0067
11.50	1.10	0.0057	1.11	0.011	1.12	0.0066

Table 2
Comparison between this work and that in [6]

State	This work		Skokov et al. [6]			
	Method A		Method A		Method B	
	E (cm^{-1})	Γ (cm^{-1})	E (cm^{-1})	Γ (cm^{-1})	E (cm^{-1})	Γ (cm^{-1})
315	19603.01	0.013	19603.17	0.00011	19603.02	0.0014
035	19610.32	0.0082	19610.50	0.067	19610.45	0.21
106	19848.38	0.0010	19848.76	0.0019	19848.78	0.000089
016	20194.38	0.00003	20194.62	0.042	20194.67	0.0042
135	20291.82	0.0014	20291.84	0.079	20291.92	0.02
415	20300.90	0.046	20300.91	0.19	20301.02	0.36
206	20573.13	0.0080	20573.41	0.0056		
306	21279.43	0.034	21279.53	0.043		
007	21714.53	0.0080	21716.33	0.012		

E is the resoanance energy or band origin and Γ is the width. The quantum numbers are as given in [6]: OCl stretch, bend, OH stretch. Method A: diagonalisation and truncation. Method B: filter diagonalisation.

stable results are a consequence of using significantly larger basis sets which is made possible by the use of a parallel computer. Our results and Skokov et al.'s agree quite well for the highest three resonances. We do not know if this observation is physically significant or simply coincidence.

The $J = 3$ calculations were performed for even ($p = 0$) rotational parity. As it is relatively quite easy to calculate the rotational constants for most of the vibrational states from $J = 1$ ro-vibrational states, we also performed $J = 1$ calculations as a guide to assignment. However the centrifugal barrier for $J = 1$ is too low to support shape resonances.

Table 3 compares resonances states with $J = 0$ and $J = 3$, $K = 0$, $p = 0$. Our calculation gives a value for the HOCl vibrational ground state rotational constant, B_0, of 0.503 cm^{-1}. Hence for the (0 0 0) state the $J = 3$, $K = 0$, $p = 0$ rotation level lies 6 cm^{-1} above the $J = 0$ state. It can be seen that the rotationally excited resonances which we identify in Table 2 generally lie 5–7 cm^{-1} above a $J = 0$ Feshbach resonance.

Just above the dissociation limit of 19289.2 cm^{-1} we find two broad ($\Gamma > 0.1$ cm^{-1}) $J = 0$ resonances at 19294.04 and 19295.10 cm^{-1}. In this region we find four narrow resonances with $J = 3$, $K = 0$, $p = 0$, which do not appear to be the counterparts of these or any other $J = 0$ resonances. These are the resonances depicted in Fig. 1 and resonance parameters for the states are given in Table 3. In this region we find 4 resonances in less than 10 cm^{-1} for $J = 3$. This should be con-

Table 3
HOCl resonance energy term values, E, and widths, Γ, for the rotational ground state and $J = 3$

$J = 0$		$J = 3$, $k = 0$, $p = 0$	
E (cm^{-1})	Γ (cm^{-1})	E (cm^{-1})	Γ (cm^{-1})
19308.75	0.0050		
19335.86	0.0064	19340.95	0.012
19402.55	0.0019	19408.00	0.0020
19424.37	0.0086	19427.20	0.0023
		19427.63	0.0021
19459.63	0.037	19468.18	0.056
19554.98	0.00072		
19603.01	0.013	19608.38	0.0066
19605.92	0.0044	19611.75	0.028
19610.32	0.0082		
19616.07	0.00099	19620.98	0.0056
19778.15	0.0068	19783.33	0.060
19848.38	0.0010	19854.25	0.0060
19874.65	0.030	19881.26	0.082
19905.91	0.0071	19911.57	0.026
19946.87	0.0018	19951.71	0.0041
20170.56	0.00052	20175.91	0.0012
20194.38	0.00003	20200.32	0.0066
20291.82	0.0014	20297.47	0.013
20300.90	0.046	20306.29	0.13
20573.13	0.0080	20578.82	0.012
20589.38	0.0013	20594.76	0.00096
20602.18	0.0056	20609.11	0.0080
20656.93	0.0011	20661.03	0.020
20868.53	0.0068	20873.38	0.0096
20897.96	0.0025	20902.05	0.013
20913.68	0.00013	20918.78	0.00019
20963.04	0.00069	20968.55	0.028
20984.56	0.0014	20989.98	0.00025
21101.69	0.00028	21105.28	0.12
21279.43	0.034	21284.98	0.0022
21332.86	0.00015	21337.98	0.035
21338.57	0.00060	21344.38	0.039
21376.02	0.0044	21381.98	0.013
21398.04	0.0025	21403.68	0.029
21464.91	0.00054	21469.97	0.0016
21690.82	0.00014	21696.63	0.0050
21714.53	0.0080	21720.62	0.0042

trasted with the $J = 0$ calculations, or indeed the $J = 3$ calculations at higher energy, where the resonances are well spaced and separated on average by more than 50 cm^{-1}. These low-lying resonances have all the characteristics of shape resonances (see Table 4).

The width of the shape resonances we identify increases systematically with energy which is consistent with more rapid tunnelling as the resonance state approaches the top of the barrier. However it would probably be unwise to read too much into this trend. In 1D problems such as the diatomic vibrator, shape resonances occur due to trapping behind a barrier in the vibrational coordinate which is also, per force, the dissociating coordinate. However a multidimensional vibrator can trap (vibrational) energy in non-dissociating degrees of freedom, yielding Feshbach resonances. The $J = 0$ states just below dissociation will vary as to their distribution of vibrational energy and one might expect the lifetimes of rotationally excited resonances associated with these states to vary accordingly.

Table 4
HOCl energy term values, E, and widths, Γ, in cm^{-1} for low-lying resonances with $J = 3$

E	Γ
19294.33	0.000015
19296.13	0.0042
19296.99	0.0082
19300.15	0.016

5. Conclusions

We have presented fully converged calculations of HOCl for $J = 0$ and $J = 3$ using an L^2 complex potential methods. We have identified a number of $J = 0$, Feshbach-type, resonance for which it is also possible to identify associated rotationally excited resonances states. In addition we have also found four low-lying rotationally excited resonances which have no resonance counterparts with $J = 0$. The 'shape' resonances have not been previously identified in above dissociation calculations on chemically bound triatomic molecules. Although the spectroscopic methods used to study HOCl (see [23]) are not well suited to the detection of shape resonance, shape resonances are known to be numerous and to play an important role in at least some near-dissociation processes [2]. The methods outlined here provide a tractable means of detecting and parameterizing these long-lived resonance states.

Acknowledgements

We thank Sergei Skokov and Joel M. Bowman for providing their potential energy surface. These calculations have been performed as part of the EPSRC ChemReact Computing Consortium.

References

[1] N. Moiseyev, Phys. Rep. 302 (1998) 211.
[2] J. Tennyson, Rep. Prog. Phys. 57 (1995) 421.
[3] E. Pollak, C. Schlier, Acc. Chem. Res. 22 (1989) 223.
[4] G. Jolicard, E.J. Austin, Chem. Phys. Lett. 121 (1985) 106.
[5] V.A. Mandelshtam, H.S. Taylor, J. Chem. Soc. Faraday Trans. 93 (1997) 847.
[6] S. Skokov, J.M. Bowman, V.A. Mandelshtam, Phys. Chem. Chem. Phys. 1 (1999) 1279.
[7] V. Ryaboy, N. Moiseyev, J. Chem. Phys. 103 (1995) 4061.
[8] H.-G. Yu, S.C. Smith, Chem. Phys. Lett. 283 (1998) 69.
[9] G. Li, H. Guo, Chem. Phys. Lett. 336 (2001) 143.
[10] J. Weiss, J. Hauschildt, S.Y. Grebenshchikov, R. Duren, R. Schinke, J. Koput, S. Stamatiadis, S.C. Farantos, J. Chem. Phys. 112 (2000) 77.
[11] J. Hauschildt, J. Weiss, C. Beck, S.Y. Grebenshchikov, R. Duren, R. Schinke, J. Koput, Chem. Phys. Lett. 300 (2001) 569.
[12] J. Hauschildt, J. Weiss, R. Schinke, Z. Phys. Chem. 214 (2000) 609.
[13] S. Skokov, J.M. Bowman, J. Chem. Phys. 111 (1999) 4933.
[14] G.S. Whittier, J.C. Light, J. Chem. Phys. 107 (1997) 1816.
[15] H.-M. Keller, R. Schinke, J. Chem. Soc. Faraday Trans. 93 (1997) 879.
[16] C.-Y. Yang, S.K. Gray, J. Chem. Phys. 107 (1997) 7773.
[17] J. Weiss, R. Schinke, V.A. Mandelshtam, J. Chem. Phys. 113 (2000) 4588.
[18] U. Brandt-Pollmann, J. Weiss, R. Schinke, J. Chem. Phys. 115 (2001) 8876.
[19] J. Weiss, R. Schinke, J. Chem. Phys. 115 (2001) 3173.
[20] J. Weiss, J. Hauschildt, R. Schinke, O. Haan, S. Skokov, J.M. Bowman, V.A. Mandelshtam, K.A. Peterson, J. Chem. Phys. 115 (2001) 8880.
[21] H.Y. Mussa, J. Tennyson, Comput. Phys. Commun. 128 (2000) 434.
[22] S. Skokov, J. Qi, J.M. Bowman, K.A. Peterson, J. Chem. Phys. 109 (1998) 2662.
[23] A. Callegari, R. Schied, P. Theulé, J. Rebstein, T.R. Rizzo, Phys. Chem. Chem. Phys. 3 (2001) 2245.
[24] J. Tennyson, J.R. Henderson, N.G. Fulton, Comput. Phys. Commun. 86 (1995) 175.
[25] H.Y. Mussa, J. Tennyson, C.J. Noble, R.J. Allan, Comput. Phys. Commun. 108 (1998) 29.
[26] H.Y. Mussa, J. Tennyson, J. Chem. Phys. 109 (1998) 10885.
[27] U.V. Riss, H.D. Meyer, J. Phys. B: At. Mol. Opt. Phys. 26 (1993) 4503.
[28] J. Tennyson, B.T. Sutcliffe, Mol. Phys. 58 (1986) 1067.
[29] J. Tennyson, J. Chem. Phys. 98 (1993) 9658.
[30] R.J. Barnes, G. Dutton, A. Sinha, J. Phys. Chem. A 101 (1997) 8374.